

Evidence-based multimodal fusion on structured EHRs and free-text notes for ICU outcome prediction

Yucheng Ruan, M.S.^{1,2}, Daniel J. Tan, M.S.², See Kiong Ng, Ph.D.², Ling Huang, Ph.D.^{1*}, Mengling Feng, Ph.D.^{1,2}

¹Saw Swee Hock School of Public Health, National University of Singapore, Singapore;

²Institute of Data Science, National University of Singapore, Singapore

ABSTRACT

Objective: Accurate Intensive Care Unit (ICU) outcome prediction is critical for improving patient treatment quality and ICU resource allocation. Existing research mainly focuses on structured data and lacks effective frameworks to integrate clinical notes from heterogeneous electronic health records (EHRs). This study aims to explore a multimodal framework based on evidence theory that can effectively combine heterogeneous structured EHRs and free-text notes for accurate and reliable ICU outcome prediction.

Materials and Methods: We proposed an evidence-based multimodal fusion framework to predict ICU outcomes, including mortality and prolonged length of stay (PLOS), by utilizing both structured EHR data and free-text notes from the MIMIC-III database. We compare the performance against baseline models that use only structured EHRs, free-text notes, or existing multimodal approaches.

Results: The results demonstrate that the evidence-based multimodal fusion model achieved both accurate and reliable prediction. Specifically, it outperformed the best baseline by 1.05%/1.02% in BACC, 9.74%/6.04% in F1 score, 1.28%/0.9% in AUROC, and 6.21%/2.68% in AUPRC for predicting mortality and PLOS, respectively. Additionally, it improved the reliability of the predictions with a 26.8%/15.1% reduction in the Brier score and a 25.0%/13.3% reduction in negative log-likelihood.

Conclusion: This study demonstrates that the evidence-based multimodal fusion framework can serve as a strong baseline for predictions using structured EHRs and free-text notes. It effectively reduces false positives, which can help improve the allocation of medical resources in the ICU. This framework can be further applied to analyze multimodal EHRs for other clinical tasks.

Keywords: Multimodal learning, Evidence fusion, Dempster-Shafer theory, ICU outcome prediction, Electronic health records

* Corresponding author: Ling Huang (huang.l@nus.edu.sg)

INTRODUCTION

The Intensive Care Unit (ICU) is a specialized hospital ward that offers comprehensive and continuous care to critically ill patients. As the population of critically ill patients grows, the demand for ICUs has risen significantly, placing strain on already limited and costly intensive care resources [1], especially during public health crises like the COVID-19 pandemic, when hospitals face an overwhelming surge of patients.

Due to the limited availability of intensive care resources, researchers have emphasized the necessity of predicting ICU outcomes such as mortality rates and prolonged lengths of stay (PLOS). Accurate predictions can help in the efficient allocation of medical resources for patients in need and reduce unnecessary expenses without compromising patient care. Furthermore, they are crucial for healthcare providers in making informed decisions about patient care strategies and providing early interventions to patients at high risk of adverse outcomes [2, 3].

Over the past two decades, the adoption of electronic ICU technology has enabled the collection of extensive data on ICU patients, creating new opportunities for developing advanced methods to predict ICU outcomes. Most previous research has concentrated on modeling ICU outcome predictions using structured EHR data [4–6], which often captures only a portion of clinical information. It may miss out on the rich contextual information that unstructured EHR data (such as nursing notes, patient narratives, and imaging reports) can provide. Natural language processing (NLP) techniques have been well explored to extract valuable insights from unstructured free-text EHR data [7–9]. Therefore, effective multimodal learning algorithms are essential to integrate heterogeneous EHRs for better ICU outcome prediction. Recently, deep learning-based multimodal models have been proven to combine structured EHR data and free-text data at the deep feature level for clinical outcome predictions [10–12]. While those methods have increased the prediction accuracy, the question regarding the reliability of those models in noisy and unstable clinical situations still exists.

In this study, we hypothesize that an effective multimodal deep neural network that incorporates both structured EHR data and free-text notes can improve the prediction of ICU outcomes. Our objective is to propose and evaluate a novel evidence-based multimodal framework for ICU outcome prediction using multimodal EHR data. Unlike traditional methods that rely on data or feature embeddings, our framework integrates information based on evidence derived from different modalities. Specifically, we use state-of-the-art deep neural networks for single-modality feature extraction: ResNet/Transformer-based models for structured EHR data and pre-trained language models for free-text EHR data. The extracted features are independently mapped into evidence and then combined in the evidence space. Experimental results on the MIMIC-III database for mortality and prolonged length of stay (PLOS) predictions demonstrate the effectiveness of the proposed model. The code implementation is available on GitHub repository (https://github.com/yuchengruan/evid_multimodal_ehr)

MATERIALS AND METHODS

Overview

In this section, we demonstrate the cohort, patient features, prediction outcomes, and proposed evidence-based multi-modal fusion framework in combining structured EHRs and free-text notes for ICU outcome prediction.

Cohort

MIMIC-III (Medical Information Mart for Intensive Care III) is a large, publicly available database containing de-identified health records from patients in critical care units at Beth Israel Deaconess Medical Center (from the US) between 2001 and 2012 [13]. We collected structured EHR data and free-text clinical notes from the database. Patients were excluded if they (1) were under 18 years of age at admission and (2) had incomplete length of stay or mortality data. For patients with multiple ICU stays, we considered only the first.

Patient features

Patient features include both structured EHR data and unstructured free-text notes. In this section, we demonstrate the patient features in our study and provide details about the data preprocessing steps.

Structured EHR data

The structured data were collected during patients' ICU stays and included demographic information, vital signs and laboratory tests, medical treatments, and comorbidities. For demographic information, the patient's age, gender, weight, ethnicity, and admission type at the time of admission were included in the study. Vital signs/lab tests are the most crucial health indicators, easily measured using non-invasive equipment, and are readily understood by all healthcare professionals. For each variable considered, we used the first value recorded within 24 hours of admission time. We then excluded any variables with $\geq 50\%$ missingness rate; this resulted in the inclusion of only heart rate among vital signs features alongside 19 lab test features, such as blood urea nitrogen, eosinophil count, and lymphocyte count, over the same period. All vital sign/lab test features were numerical variables. Medical treatments, which include services and interventions provided to patients and recorded in digital systems, were also analyzed. Treatments such as sedatives, statins, diuretics, antibiotics, ventilation, and vasopressors were included, with each treatment feature coded as a binary variable, indicating whether the patient received the treatment. Comorbidities refer to the presence of additional medical conditions, which play a role in decision-making models. In this study, comorbidities such as hypertension, diabetes, alcohol abuse, cerebrovascular accident (stroke), congestive heart failure, and ischemic heart disease were included, all represented as binary variables.

All categorical features were encoded using one-hot encoding, and numerical features were normalized. Missing data were addressed by imputing the mean for continuous features and the mode for categorical features, ensuring data consistency. Eventually, the structured data contained 41 features.

Free-text EHR notes

Free-text notes contain a rich repository of clinical information about observations, assessments, and the overall clinical picture, which structured data often fails to capture. Furthermore, they provide an important context for interpreting structured data. For instance, while lab results may indicate abnormal values, free-text notes can clarify the relevance of these results by considering the patient’s history, comorbidities, or specific circumstances at the time of testing. As a result, NLP techniques, especially pre-trained LLM, can be applied to these notes to gain deeper insights for data-driven predictions. In this study, we focus on *Nursing*, *Nursing/Other*, *Physician*, and *Radiology* notes, as these comprise the majority of clinical documentation and are frequently recorded in the MIMIC-III database [10]. We extracted only the first 24 hours of notes for each admission to facilitate early outcome prediction.

All notes were preprocessed by appending the feature name at the front to help the pre-trained language model better understand the clinical texts. For instance, if the content $[x]$ of a note is under *Nursing*, the processed note would be *Nursing: [x]*. The four types of notes were then concatenated using a newline symbol ($\backslash n$) to form a unified *Notes* for each patient. Tokenizers from pre-trained language models in Huggingface were employed to break the notes into tokens, standardizing the free-text data for further NLP tasks. The *Notes* was transformed to a fixed length of 512 tokens to ensure input consistency; longer notes were truncated, while shorter notes were padded.

Prediction Outcomes

In this study, we focus on two ICU prediction outcomes: mortality and prolonged length of stay.

Mortality

Mortality is widely acknowledged as a critical outcome in ICUs. The primary objective of this task is to determine whether a patient is likely to die during their hospital stay. Accurate predictions enable the early identification of high-risk patients and support the efficient allocation of ICU resources. This prediction task is typically framed as a binary classification problem, with the label indicating the occurrence or absence of a death event.

Prolonged length of stay

Length of stay refers to the duration between a patient’s admission to and discharge from the ICU. In this study, we aim to predict prolonged length of stay (PLOS), defined as a stay exceeding 7 days [10, 14, 15]. Prolonged ICU stays are often linked to severe illnesses, complications, and increased mortality. Moreover, they place considerable pressure on hospital resources by reducing the availability of ICU beds and specialized personnel. Efficient management of ICU LOS not only improves patient outcomes but also enhances the overall effectiveness of healthcare systems. This problem is framed as a binary classification task.

Model architecture

The overview of the proposed framework is illustrated in Figure 1. In general, we propose to generate the modality-level evidence for both structured data and free-text notes using the evidence mapping module and fuse the modality-

level evidence for final prediction.

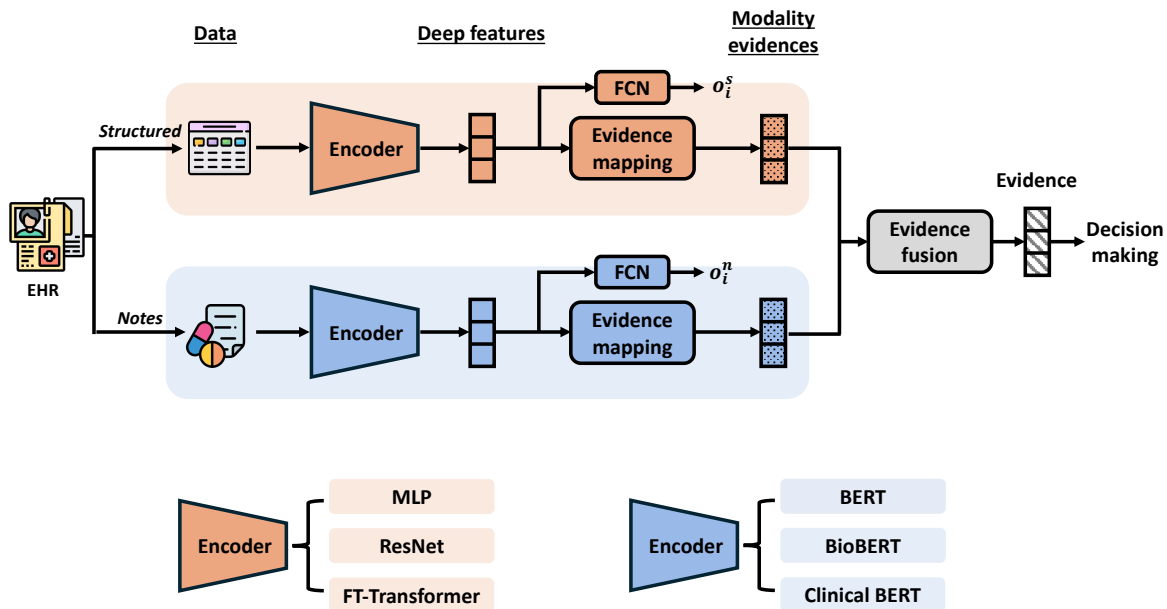


Figure 1: The overview of our proposed framework. EM: evidence mapping and EF: evidence fusion

Evidence mapping (EM)

Denœux [16] proposed an evidential neural network (ENN) that maps imperfect (uncertain, imprecise, or noise) input features into degrees of belief and ignorance (uncertainty) under the framework of Dempster-Shafer (DS) theory [17, 18]. The essential concept of ENN is to consider each prototype as a piece of evidence, which is discounted based on its distance from the input vector. The evidence from different prototypes is then aggregated using Dempster’s combination rule. Inspired by ENN and its promising adoptions in medical data analysis [19–22], we propose incorporating ENN as an evidence mapping module with the state-of-the-art encoders to generate evidence for structured EHRs and free-text notes. Further details about DS theory and evidence mapping can be found in Appendix A and B. Given modality level input, the evidence mapping module can output the evidence for each class as well as the uncertainty regarding this prediction.

Structured data evidence mapping To produce modality evidence for structured data, we initially used a structured data encoder to extract deep features (the output dimension is set to 32). We considered three popular encoders to extract the embeddings: MLP, ResNet, FT-Transformer [23] (see Baselines section for more details). Subsequently, we introduced an evidence mapping module to transform the deep features into evidence embeddings for structured data.

Free-text notes evidence mapping Similarly, we utilized pre-trained language models to extract the deep features from clinical notes, on which we developed an evidence mapping module to produce the evidence of the modality. Our primary analysis focused on pre-trained architectures similar to BERT. Accordingly, three BERT-based architectures were evaluated: BERT [24], BioBERT [24], Clinical BERT [25] (see Baselines section for more details). To minimize

computational overhead while maintaining high predictive performance, we froze the pre-trained language models and fine-tuned an additional layer (128 hidden units) on top in model training.

Evidence fusion (EF)

Based on the modality-level evidence obtained from structured EHR and free-text notes, we developed the evidence fusion module based on Dempster’s combination rule to generate the final evidence for decision-making. Further details about the fusion of EHR and free-text notes evidence can be found in Appendix C.

Augmented learning algorithm

We optimize the proposed framework using an augmented learning algorithm, which includes two types of optimization objectives: (1) main objective and (2) auxiliary objective. The main objective is to optimize predictive performance based on transformed evidence as the primary loss function. Additionally, two auxiliary cross-entropy losses are incorporated to enhance the feature representation capability of the independent encoders for the two modalities, as the evidence mapping module performs more effectively with high-quality representations. More details can be found in the Appendix D.

Evaluation and experiment

Baselines

To comprehensively evaluate the effectiveness of our proposed fusion framework, we employed three types of classification models as baselines: (1) models with structured data only, (2) models with free-text notes only, and (3) existing multimodal models based on both data. The configurations for the structured data models are as follows:

Random Forest [26]: A decision tree-based ensemble learning method for making predictions.

MLP [23]: A fundamental neural network with fully connected layers to encode structured data and serves as a reliable baseline. The model was configured with 3 layers, 32 hidden units, and a dropout rate of 0.1.

ResNet [23]: Because of the success of ResNet in computer vision [27], it has also been adapted for structured data modeling. Specifically, the main building block is simplified by providing a direct path from input to output. The configuration in our study has 3 residual blocks, 32 hidden units, and a dropout rate of 0.1.

FT-Transformer [23]: It converts all categorical and numerical features into embeddings, which are then processed through a couple of Transformer layers. It has demonstrated superior performance as a structured data encoder across various tasks. The model configuration has 3 Transformer layers with 192 hidden units, 8 attention heads, and a dropout rate of 0.2.

As our focus is on pre-trained language models similar to BERT, we employed three BERT-based text classification models in this study:

BERT [24]: a pre-trained large language model English corpus using a self-supervised approach. Through masked language modeling and next-sentence prediction objectives, the model learns internal representations of the English

language, enabling it to extract features useful for downstream tasks. In this study, we utilized the *google-bert/bert-base-uncased* model from Huggingface [28] for feature extraction.

BioBERT [29]: a variant of BERT pre-trained on biomedical literature, such as PubMed abstracts, and is optimized to perform more effectively on biomedical NLP tasks. In this study, we used *dmis-lab/biobert-v1.1* from Huggingface as the extraction model.

Clinical BERT [25]: A fine-tuned version of BERT on clinical notes from the MIMIC-III database, making it well-suited for handling medical terminology and clinical narratives to enhance performance on clinical tasks. In our study, we used *emilyalsentzer/Bio_ClinicalBERT* from the Huggingface transformer library for extracting embeddings from clinical notes.

We also implemented a Multimodal approach for the ICU outcome prediction from [12]: it concatenated the structured EHRs with the extracted embeddings from free-text notes, which were then passed into 2 fully connected layers for prediction. It supports different text encoders, and in this study, we used BERT, BioBERT, and Clinical BERT for fair comparisons

Implementation details

The dataset was randomly divided with 60% for training, 20% for validation, and 20% for testing. For model training, a mini-batch size of 32 was used, and the maximum number of epochs was set to 150, with early stopping applied. Each model was trained five times with different random seeds, and we reported the average results along with the standard error of the metrics to ensure statistical reliability. Hyperparameters were optimized for all baseline models to achieve the best results.

All compared models were implemented using Scikit-learn [30], PyTorch [31], and Hugging Face's Transformers library [28] in Python 3.8.19. The MLP, ResNet, and FT-Transformer models were built using the original source code on GitHub (<https://github.com/yandex-research/rtdl-revisiting-models>). The Multimodal approach was modified based on the code on Github (https://github.com/WeiChunLin/Bio_Clinical_BERT_Multimodal_Model).

Model evaluation

For comprehensive model evaluation and comparison, we reported the following metrics: precision, recall, specificity, negative predictive value (NPV), balanced accuracy (BACC), F1 score, area under the receiver operating characteristic curve (AUROC), area under the precision-recall curve (AUPRC), Brier score, and negative log-likelihood (NLL). Precision, recall, specificity, and NPV assess model performance for positive or negative samples. In contrast, BACC, F1 score, AUROC, and AUPRC provide a more holistic evaluation of predictive performance. Meanwhile, the Brier score and NLL measure the prediction reliability.

Other fusion settings

In addition to fusing evidence from modalities (structured EHRs and free-text notes), we evaluated our framework under two additional fusion settings: data types and data sources. The illustration is shown in Figure 2.

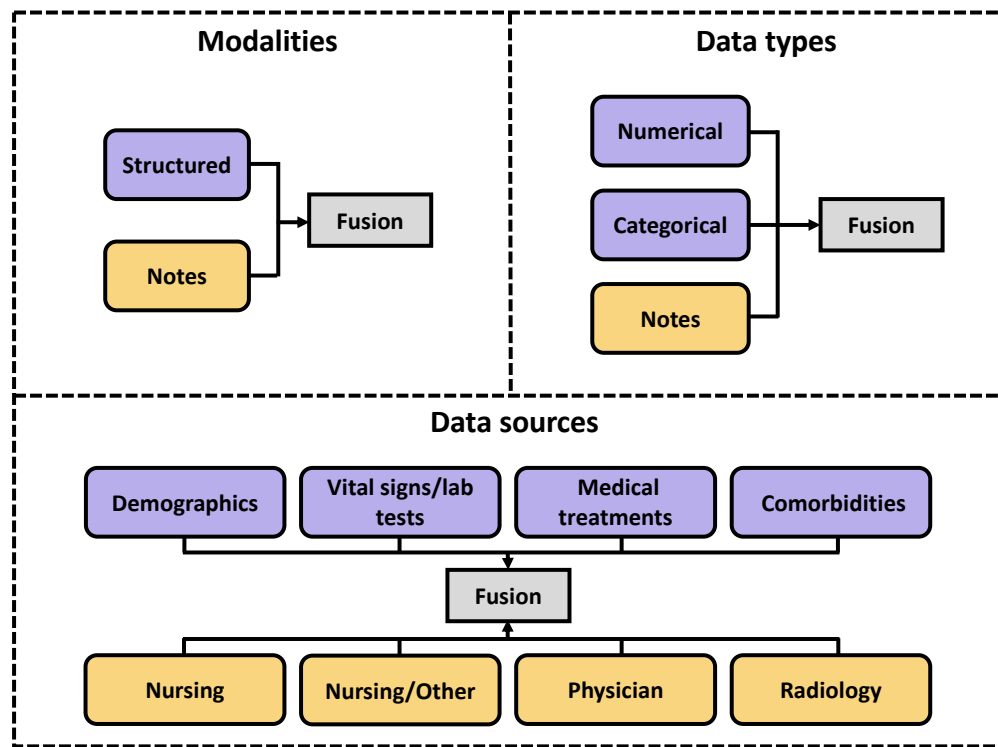


Figure 2: The illustration of different fusion settings.

Data types: Features can be grouped based on their data types. In our study, we further divided the structured data into two types: numerical and categorical data.

Data Sources: Features can also be grouped according to their sources. In our case, the structured data was split into four sources: demographics, vital signs/lab tests, medical treatments, and comorbidities. Similarly, we categorized the clinical notes into four types: Nursing, Nursing/Other, Physician, and Radiology notes. For each group, we generated evidence using individual encoders and evidential layers. These pieces of evidence were then aggregated through the EF module to produce the final evidence for decision-making.

RESULTS

Data description

Table 1 shows the descriptive characteristics of the patients in the study cohort. Our cohort includes 38469 patients in total under the inclusion criteria, in which 4540 (11.8%) patients were identified as dead during the stay while 5220 (13.6%) patients were identified as having prolonged length of stay. The patient demographic showed that the majority of patients were white, and male patients were slightly more than the female. Most of the admitted patients in the ICU were identified as emergency. Over half (51.2%) of patients received mechanical ventilation during their ICU stay and hypertension (38.8%) and congestive heart failure (31.2%) were among the most common patient comorbidities.

Patient characteristic	Mortality		PLOS	
	Yes (N=4540)	No (N=33928)	Yes (N=5220)	No (N=33248)
Age	68.6 (15.1)	61.6 (16.9)	62.9 (16.3)	62.3 (16.9)
Gender				
Male	2399 (52.8%)	19378 (57.1%)	2943 (56.4%)	18834 (56.6%)
Female	2141 (47.2%)	14550 (42.9%)	2277 (43.6%)	14414 (43.4%)
Weight	79.1 (22.7)	83.0 (23.1)	84.6 (24.3)	82.2 (22.9)
Ethnicity				
White	3100 (68.3%)	24343 (71.7%)	3661 (70.1%)	23782 (71.5%)
Black	260 (5.7%)	2688 (7.9%)	354 (6.8%)	2594 (7.8%)
Asian	106 (2.3%)	1166 (3.4%)	153 (2.9%)	1101 (3.3%)
Hispanic	88 (1.9%)	803 (2.4%)	104 (2.0%)	805 (2.4%)
Other/Unknown	986 (21.7%)	4928 (14.5%)	948 (18.2%)	4966 (14.9%)
Admission type				
Emergency	4240 (93.4%)	27062 (79.8%)	4480 (85.8%)	26822 (80.7%)
Elective	165 (3.6%)	5911 (17.4%)	533 (10.2%)	5543 (16.7%)
Urgent	135 (3.0%)	955 (2.8%)	207 (4.0%)	883 (2.7%)
Heart rate	91.4 (22.0)	86.8 (18.7)	91.5 (21.0)	86.7 (18.8)
APTT	39.7 (27.1)	34.7 (21.6)	37.2 (23.8)	35.0 (22.2)
BUN	34.1 (25.1)	23.8 (19.0)	28.1 (22.3)	24.5 (19.7)
Eosinophil	1.3 (3.1)	1.5 (1.9)	1.2 (1.7)	1.5 (2.1)
Lymphocytes	12.1 (11.9)	15.5 (11.4)	12.5 (10.8)	15.4 (11.6)
Neutrophils	77.3 (17.7)	76.6 (13.9)	77.8 (15.2)	76.5 (14.4)
RDW	15.5 (2.4)	14.5 (1.9)	14.9 (2.1)	14.6 (2.0)
Bicarbonate	22.6 (5.7)	24.3 (4.4)	23.6 (5.2)	24.1 (4.5)
Chloride	103.3 (7.3)	104.1 (6.0)	104.0 (6.7)	104.0 (6.1)
Creatinine	1.6 (1.4)	1.3 (1.4)	1.4 (1.5)	1.3 (1.4)
Hemoglobin	11.3 (2.3)	11.8 (2.3)	11.6 (2.2)	11.7 (2.3)
Mean cell volume	91.5 (7.7)	89.4 (6.6)	90.3 (7.1)	89.6 (6.7)
Platelet count	227.2 (132.2)	239.0 (112.3)	231.8 (119.8)	238.5 (114.0)
Potassium	4.3 (0.9)	4.2 (0.7)	4.2 (0.8)	4.2 (0.7)
Sodium	138.2 (6.2)	138.6 (4.6)	138.7 (5.2)	138.5 (4.7)
PT	17.4 (10.6)	15.1 (6.8)	16.0 (8.2)	15.3 (7.3)
INR	1.8 (2.2)	1.4 (1.3)	1.6 (1.9)	1.4 (1.4)
WBC	14.3 (16.5)	11.5 (8.8)	12.9 (8.8)	11.6 (10.2)
PLR	39.9 (56.7)	30.4 (47.4)	38.4 (57.5)	30.6 (47.3)
NLR	13.9 (15.6)	9.9 (13.7)	13.0 (15.2)	10.1 (13.8)
Sedatives	1263 (27.8%)	9114 (26.9%)	2360 (45.2%)	8017 (24.1%)
Statin	405 (8.9%)	5164 (15.2%)	556 (10.7%)	5013 (15.1%)
Diuretic	567 (12.5%)	5435 (16.0%)	865 (16.6%)	5137 (15.5%)
Antibiotics	952 (21.0%)	4836 (14.3%)	1122 (21.5%)	4666 (14.0%)
Ventilation	2326 (51.2%)	10923 (32.2%)	3105 (59.5%)	10144 (30.5%)
Vasopressor	1538 (33.9%)	6340 (18.7%)	1639 (31.4%)	6239 (18.8%)
Hypertension	1760 (38.8%)	16221 (47.8%)	2199 (42.1%)	15782 (47.5%)
Diabetes	1107 (24.4%)	9249 (27.3%)	1401 (26.8%)	8955 (26.9%)
Alcohol abuse	202 (4.4%)	1554 (4.6%)	333 (6.4%)	1423 (4.3%)
CVA	309 (6.8%)	1139 (3.4%)	364 (7.0%)	1084 (3.3%)
CHF	1416 (31.2%)	8711 (25.7%)	1867 (35.8%)	8260 (24.8%)
IHD	1276 (28.1%)	12390 (36.5%)	1634 (31.3%)	12032 (36.2%)

Table 1: Characteristics of structured features in the patient cohort. For categorical features, the number of instances in each category is reported along with the percentage. For continuous features, the mean and standard deviation are reported in the study.

Model	Structured	Notes	BACC \uparrow	F1 \uparrow	AUROC \uparrow	AUPRC \uparrow	Brier \downarrow	NLL \downarrow
Random Forest	x		0.7172 \pm 0.0019	0.3820 \pm 0.0018	0.7988 \pm 0.0010	0.3766 \pm 0.0030	0.1891 \pm 0.0006	0.5639 \pm 0.0015
MLP	x		0.7486 \pm 0.0003	0.4043 \pm 0.0019	0.8326 \pm 0.0011	0.4429 \pm 0.0033	0.1677 \pm 0.0015	0.4937 \pm 0.0037
ResNet	x		0.7521 \pm 0.0011	0.4113 \pm 0.0007	0.8350 \pm 0.0006	0.4468 \pm 0.0016	0.1654 \pm 0.0006	0.4895 \pm 0.0015
FT-Transformer	x		0.7592 \pm 0.0025	0.4166 \pm 0.0021	0.8426 \pm 0.0013	0.4577 \pm 0.0029	0.1648 \pm 0.0014	0.4832 \pm 0.0037
BERT		x	0.6300 \pm 0.0014	0.2814 \pm 0.0019	0.6777 \pm 0.0014	0.2037 \pm 0.0012	0.2302 \pm 0.0070	0.6523 \pm 0.0159
BioBERT		x	0.6164 \pm 0.0043	0.2759 \pm 0.0021	0.6695 \pm 0.0016	0.2181 \pm 0.0009	0.2214 \pm 0.0021	0.6326 \pm 0.0048
Clinical Bert		x	0.6614 \pm 0.0007	0.3080 \pm 0.0009	0.7240 \pm 0.0001	0.2928 \pm 0.0008	0.2132 \pm 0.0030	0.6086 \pm 0.0070
Multimodal (BERT)	x	x	0.7531 \pm 0.0016	0.4079 \pm 0.0031	0.8398 \pm 0.0006	0.4596 \pm 0.0021	0.1691 \pm 0.0030	0.4992 \pm 0.0077
Multimodal (BioBERT)	x	x	0.7558 \pm 0.0007	0.4073 \pm 0.0027	0.8362 \pm 0.0006	0.4570 \pm 0.0032	0.1725 \pm 0.0028	0.5084 \pm 0.0088
Multimodal (Clinical Bert)	x	x	0.7584 \pm 0.0005	0.4218 \pm 0.0019	0.8404 \pm 0.0004	0.4686 \pm 0.0026	0.1606 \pm 0.0022	0.4792 \pm 0.0046
Ours (MLP-BERT)	x	x	0.7525 \pm 0.0030	0.4466 \pm 0.0042	0.8406 \pm 0.0010	0.4764 \pm 0.0020	0.1345 \pm 0.0050	0.4041 \pm 0.0128
Ours (MLP-BioBERT)	x	x	0.7492 \pm 0.0042	0.4493 \pm 0.0060	0.8408 \pm 0.0012	0.4758 \pm 0.0009	0.1301 \pm 0.0062	0.3927 \pm 0.0159
Ours (MLP-Clinical Bert)	x	x	0.7467 \pm 0.0022	0.4629\pm0.0033	0.8465 \pm 0.0008	<u>0.4935\pm0.0011</u>	0.1176\pm0.0027	0.3594\pm0.0066
Ours (ResNet-BERT)	x	x	0.7581 \pm 0.0037	0.4404 \pm 0.0038	0.8415 \pm 0.0011	0.4688 \pm 0.0014	0.1435 \pm 0.0052	0.4296 \pm 0.0133
Ours (ResNet-BioBERT)	x	x	0.7546 \pm 0.0039	0.4438 \pm 0.0053	0.8424 \pm 0.0012	0.4671 \pm 0.0014	0.1392 \pm 0.0061	0.4187 \pm 0.0157
Ours (ResNet-Clinical Bert)	x	x	0.7580 \pm 0.0023	0.4472 \pm 0.0042	0.8474 \pm 0.0006	0.4899 \pm 0.0015	0.1387 \pm 0.0043	0.4178 \pm 0.0110
Ours (FT-Trans-BERT)	x	x	<u>0.7634\pm0.0012</u>	0.4432 \pm 0.0060	0.8485 \pm 0.0007	0.4797 \pm 0.0029	0.1450 \pm 0.0049	0.4345 \pm 0.0129
Ours (FT-Trans-BioBERT)	x	x	0.7610 \pm 0.0015	0.4507 \pm 0.0007	<u>0.8486\pm0.0011</u>	0.4796 \pm 0.0027	0.1358 \pm 0.0014	0.4095 \pm 0.0045
Ours (FT-Trans-Clinical Bert)	x	x	0.7672\pm0.0032	<u>0.4541\pm0.0032</u>	0.8534\pm0.0012	0.4977\pm0.0011	0.1390 \pm 0.0043	0.4192 \pm 0.0112

(a) Mortality prediction

Model	Structured	Notes	BACC \uparrow	F1 \uparrow	AUROC \uparrow	AUPRC \uparrow	Brier \downarrow	NLL \downarrow
Random Forest	x		0.6680 \pm 0.0025	0.3492 \pm 0.0038	0.7270 \pm 0.0018	0.2980 \pm 0.0029	0.2350 \pm 0.0009	0.6649 \pm 0.0018
MLP	x		0.6845 \pm 0.0009	0.3736 \pm 0.0011	0.7528 \pm 0.0010	0.3353 \pm 0.0010	0.1950 \pm 0.0018	0.5739 \pm 0.0044
ResNet	x		0.6851 \pm 0.0017	0.3774 \pm 0.0018	0.7532 \pm 0.0004	0.3366 \pm 0.0021	0.1929 \pm 0.0012	0.5702 \pm 0.0027
FT-Transformer	x		0.6956 \pm 0.0011	0.3790 \pm 0.0021	0.7674 \pm 0.0006	0.3404 \pm 0.0021	0.1947 \pm 0.0031	0.5704 \pm 0.0079
BERT		x	0.6087 \pm 0.0011	0.2960 \pm 0.0016	0.6507 \pm 0.0015	0.2262 \pm 0.0009	0.2316 \pm 0.0043	0.6557 \pm 0.0091
BioBERT		x	0.6057 \pm 0.0016	0.2940 \pm 0.0012	0.6487 \pm 0.0014	0.2214 \pm 0.0012	0.2297 \pm 0.0029	0.6518 \pm 0.0063
Clinical Bert		x	0.6420 \pm 0.0016	0.3261 \pm 0.0015	0.6946 \pm 0.0009	0.2661 \pm 0.0006	0.2225 \pm 0.0031	0.6350 \pm 0.0069
Multimodal (BERT)	x	x	0.6903 \pm 0.0018	0.3739 \pm 0.0012	0.7625 \pm 0.0006	0.3427 \pm 0.0007	0.2017 \pm 0.0028	0.5960 \pm 0.0082
Multimodal (BioBERT)	x	x	0.6905 \pm 0.0022	0.3731 \pm 0.0025	0.7606 \pm 0.0007	0.3364 \pm 0.0009	0.1974 \pm 0.0026	0.5888 \pm 0.0043
Multimodal (Clinical Bert)	x	x	0.6933 \pm 0.0014	0.3714 \pm 0.0023	0.7648 \pm 0.0009	0.3544 \pm 0.0018	0.2027 \pm 0.0056	0.5871 \pm 0.0136
Ours (MLP-BERT)	x	x	0.6878 \pm 0.0016	0.3868 \pm 0.0030	0.7580 \pm 0.0004	0.3499 \pm 0.0015	0.1773 \pm 0.0022	0.5288 \pm 0.0063
Ours (MLP-BioBERT)	x	x	0.6866 \pm 0.0022	0.3905 \pm 0.0038	0.7573 \pm 0.0010	0.3461 \pm 0.0023	0.1720 \pm 0.0031	0.5172 \pm 0.0076
Ours (MLP-Clinical Bert)	x	x	0.6870 \pm 0.0012	0.3952 \pm 0.0032	0.7633 \pm 0.0008	0.3557 \pm 0.0021	0.1637\pm0.0054	0.4943\pm0.0145
Ours (ResNet-BERT)	x	x	0.6931 \pm 0.0013	0.3887 \pm 0.0040	0.7655 \pm 0.0011	<u>0.3584\pm0.0007</u>	0.1815 \pm 0.0045	0.5398 \pm 0.0107
Ours (ResNet-BioBERT)	x	x	0.6896 \pm 0.0011	0.3918 \pm 0.0037	0.7647 \pm 0.0009	0.3532 \pm 0.0010	0.1752 \pm 0.0048	0.5241 \pm 0.0123
Ours (ResNet-Clinical Bert)	x	x	0.6974 \pm 0.0011	0.4019\pm0.0015	0.7705 \pm 0.0009	0.3639\pm0.0010	<u>0.1694\pm0.0018</u>	<u>0.5082\pm0.0042</u>
Ours (FT-Trans-BERT)	x	x	<u>0.7005\pm0.0010</u>	0.3809 \pm 0.0024	<u>0.7725\pm0.0006</u>	0.3524 \pm 0.0011	0.1927 \pm 0.0039	0.5617 \pm 0.0100
Ours (FT-Trans-BioBERT)	x	x	0.6986 \pm 0.0011	0.3847 \pm 0.0030	<u>0.7701\pm0.0012</u>	0.3504 \pm 0.0014	0.1832 \pm 0.0045	0.5376 \pm 0.0113
Ours (FT-Trans-Clinical Bert)	x	x	0.7027\pm0.0011	<u>0.3942\pm0.0020</u>	0.7743\pm0.0006	0.3575 \pm 0.0014	0.1760 \pm 0.0018	0.5205 \pm 0.0038

(b) PLOS prediction

Table 2: The model comparison for mortality (a) and PLOS prediction (b) tasks.

Model performance

Table 2 presents the comparison of model performance under predictive evaluation metrics (BACC, F1 score, AUROC, and AUPRC) and reliability evaluation metrics (Brier score and NLL) for both mortality prediction (2a) and PLOS (2b) prediction tasks. The comparison results under precision, recall, specificity, and NPV can be found in Appendix E.

Overall, our framework demonstrated superior performance across both tasks. In the mortality prediction task, our framework using MLP and Clinical BERT as the backbone achieved the highest F1 score (0.4629) and the lowest Brier score (0.1176) and NLL (0.3594). Furthermore, with FT-Transformer and Clinical BERT, it achieved the highest balanced accuracy (BACC) of 0.7672, AUROC of 0.8534, and AUPRC of 0.4977. Compared to the best baseline models, our framework improved predictive performance by approximately 1.05% in BACC, 9.74% in F1 score, 1.28% in AUROC, and 6.21% in AUPRC. Additionally, it significantly enhanced prediction reliability, with reductions of about 26.8% in Brier score and 25.0% in NLL.

In the PLOS prediction task, our framework demonstrated exceptional performance across all key predictive evaluation metrics, achieving a BACC of 0.7027, an F1 score of 0.4019, an AUROC of 0.7743, and an AUPRC of 0.3639.

Compared to the best baseline model, our framework showed notable improvements: a 1.02% increase in BACC, a 6.04% increase in F1 score, a 0.9% increase in AUROC, and a 2.68% increase in AUPRC. Additionally, it enhanced prediction reliability with a 15.1% reduction in Brier score and a 13.3% reduction in NLL.

Models that relied solely on structured data or free-text notes underperformed compared to our proposed framework in both predictive and reliability evaluation metrics. While the multimodal approach showed marginally better performance than other baselines in the mortality prediction task, it delivered weaker results in the PLOS prediction task.

Evaluation on different fusion settings

Figure 3 illustrates the evaluation of our framework across three fusion settings applied to different backbone models for mortality prediction. For the corresponding results in the PLOS prediction task, please refer to Appendix F. Both tasks exhibited similar patterns in the analysis.

Regarding predictive evaluation metrics, the models achieved comparable BACC across the three fusion settings for both tasks. Notably, the model based on modalities outperformed those based on data types and data sources in F1, AUROC, and AUPRC metrics. In terms of reliability evaluation metrics, the model based on modalities demonstrated superior reliability across different backbone models.

DISCUSSION

Principle findings

In this section, we present our findings across four key areas: the advantages of using free-text notes for mortality and PLOS prediction, the effectiveness of evidence-based multimodal framework, the impact of various fusion settings, and the influence of encoder selection.

Benefits of free-text notes

From Table 2, it is evident that integrating free-text notes with structured data enhances ICU outcome prediction, boosting predictive performance and reliability. Free-text notes provide information not included in structured EHR data, such as nursing details, physician documentation, and radiology reports after ICU admission. This suggests that free-text EHR notes and structured inputs can complement each other in predictive modeling, leading to improved performance.

Effectiveness of evidence-based multimodal framework

Our evidence-based framework demonstrated improved predictive performance and higher reliability compared to existing multimodal approaches. This improvement is likely due to the heterogeneous nature of EHRs, which often contain imprecise information from diverse sources. By effectively extracting and integrating informative evidence through modalities, our framework addresses these challenges.

Additionally, the current multimodal approach achieved higher recall in both tasks (refer to Appendix E). High recall

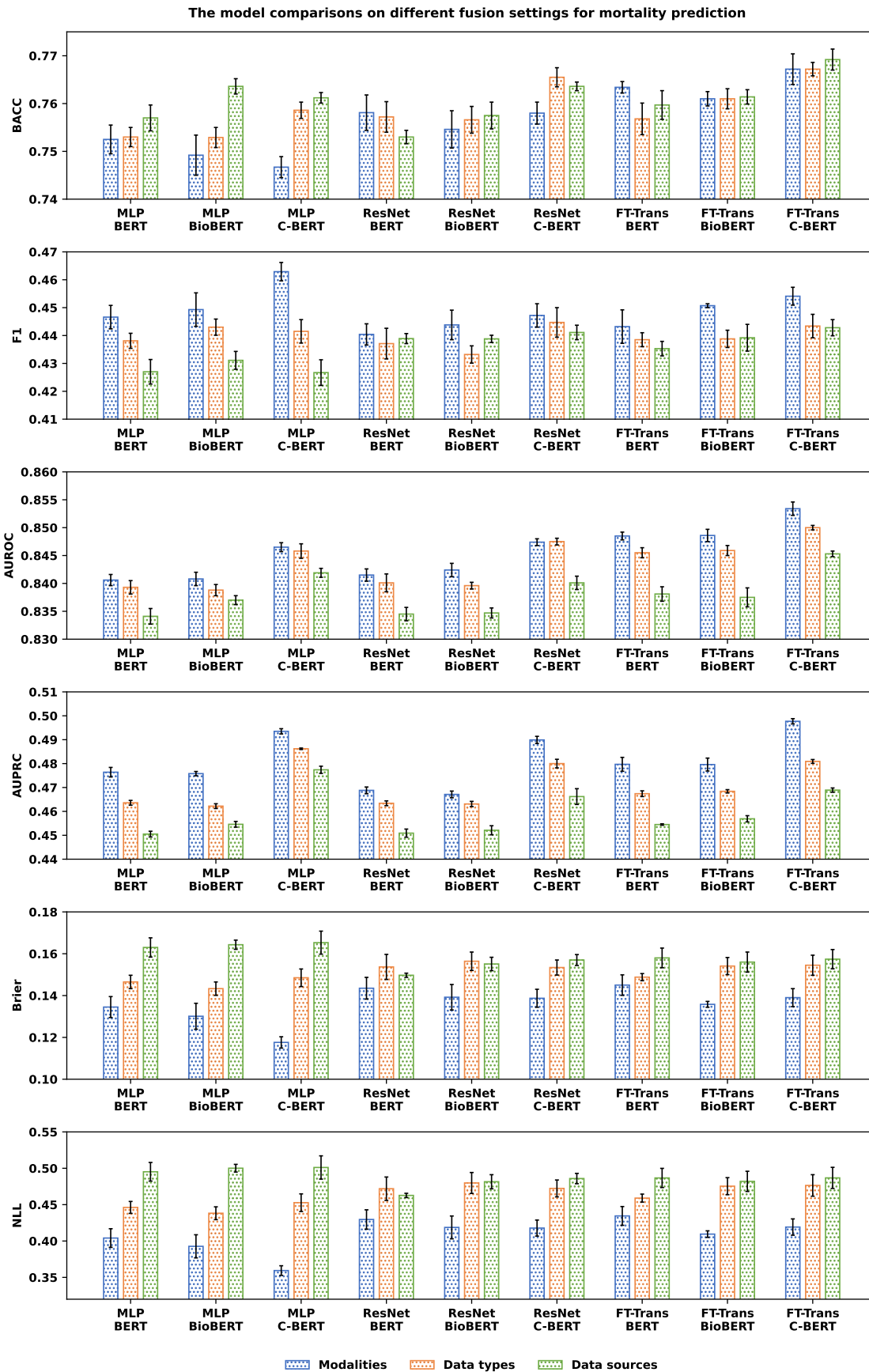


Figure 3: The evaluation of our framework on different fusion settings for mortality prediction: (1) modalities, (2) data types, (3) data sources.

reflects the model's ability to capture the most true positive instances, often at the cost of accepting more false positives. In ICU settings, this could result in the unnecessary utilization of medical resources and equipment. In contrast, our framework strikes a better balance by demonstrating higher precision and specificity, reducing false positives. This capability is critical to appropriately allocate medical resources to ICU patients in real need.

It is also noteworthy that the improvement in BACC (1.05% for mortality prediction and 1.02% for PLOS prediction) is smaller than the improvement in F1 score (9.74% for mortality prediction and 6.04% for PLOS prediction). The F1 score, which emphasizes the balance between precision and recall, is particularly valuable for assessing improvements in identifying positive samples within imbalanced datasets, especially when positive outcomes are rare. Given that ICU outcomes are a minority in our dataset, this suggests that our framework is particularly effective at correctly identifying these critical outcomes.

Impacts of different fusion settings

To explore the performance of our framework across different fusion settings, it is evident that models based on modalities achieved higher F1 scores but lower BACCs compared to the other two fusion settings. This discrepancy arises from the metrics' focus: the F1 score emphasizes performance on the positive class by balancing precision and recall, while balanced accuracy (BACC) provides an overall assessment of recall across all classes. Thus, models based on modalities are more effective at identifying ICU outcomes, likely due to the enhanced integration of information from independent sources facilitated by evidence theory.

This observation aligns with our analysis of data independence. Figures 4 and 5 visualize the independence of structured features and four types of free-text notes, respectively. In Figure 4, correlation coefficients confirm that features within structured data are not independent. Meanwhile, Figure 5 shows that Radiology notes form a distinct cluster, while the other types of notes overlap, indicating a lack of independence among them. Additionally, our analysis highlights a general relationship between predictive performance and reliability.

Influence of encoders selection

The evaluations presented in Tables 2 and 3 reveal that the choice of encoders plays a critical role in determining predictive performance. Among the models assessed, the FT-Transformer stands out as highly effective for tabular data, aligning with the findings of [23]. This effectiveness can be attributed to the transformer's capability to capture complex relationships among transformed numerical and categorical features, which enhances its predictive power.

For pre-trained language encoders, Clinical BERT demonstrates the best performance in extracting clinical information from free-text notes. Its superiority stems from its unique pre-training on clinical text from the MIMIC-III database. This specialized pre-training enables Clinical BERT to generate more informative embeddings by leveraging its pre-learned clinical knowledge and domain-specific term embeddings, resulting in improved model performance.

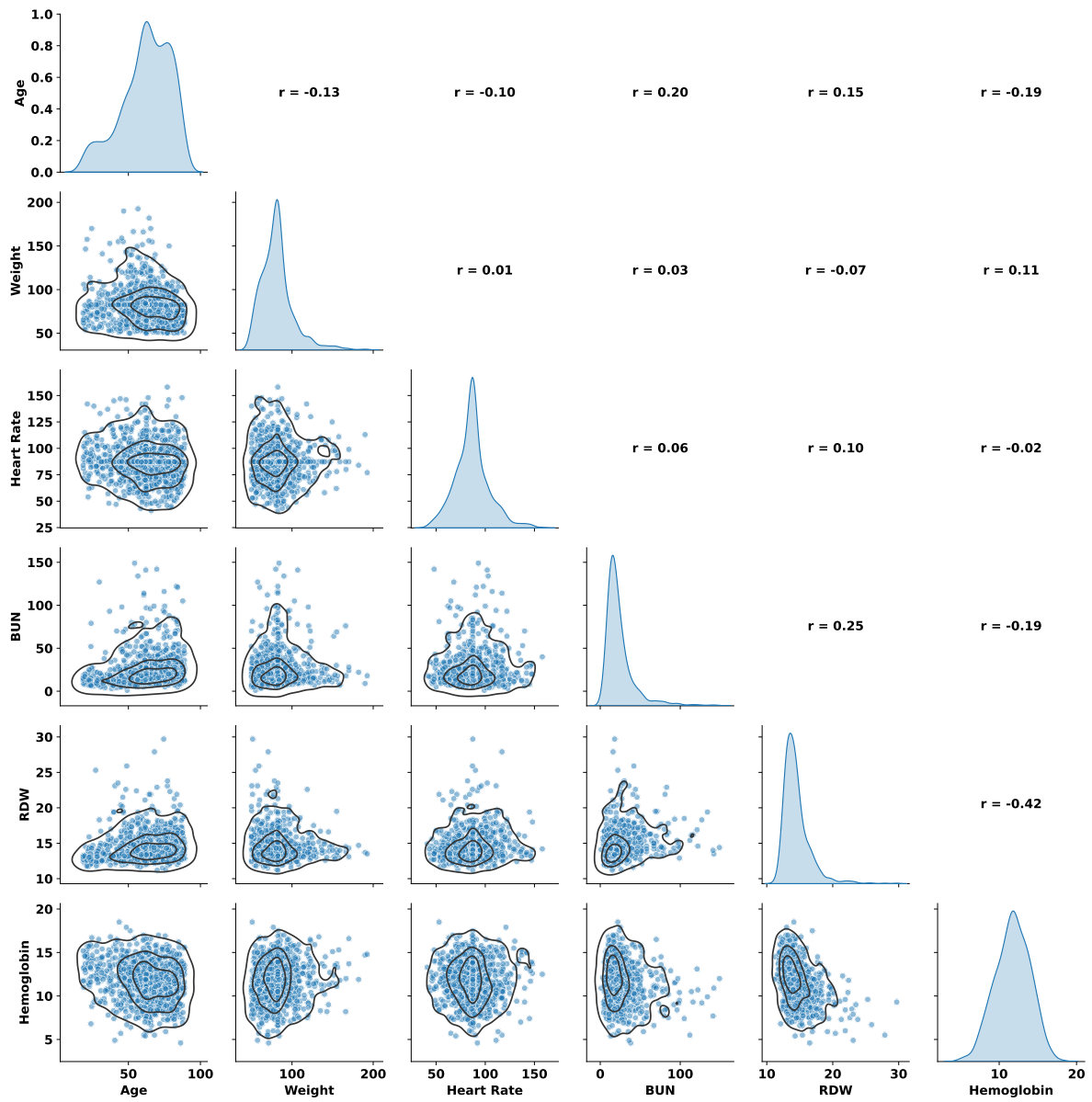


Figure 4: The pair plots and correlation coefficients of some structured features from different sources.

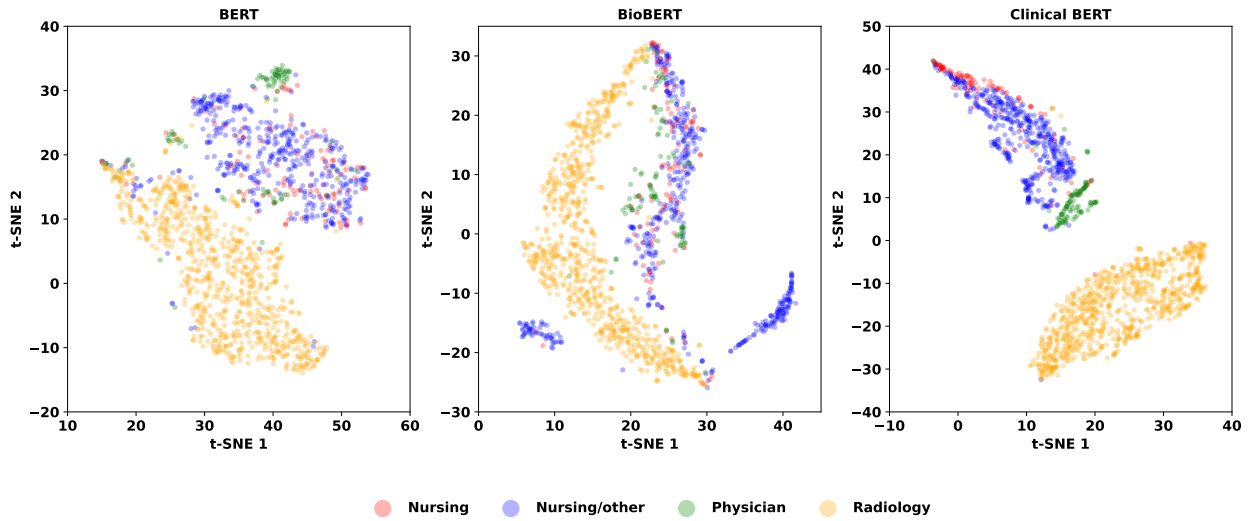


Figure 5: The t-SNE visualization on extracted embeddings of four different types of free-texts in EHRs: Nursing, Nursing/other, Physician, Radiology.

CONCLUSION

In this paper, we address the challenge of predicting ICU outcomes by introducing an evidence-based multimodal framework that models both structured EHR data and free-text EHR notes. Our framework transforms deep features extracted from these two modalities into evidence through evidence mapping module, which is then fused using Dempster’s rule to make final predictions. Through experiments on the MIMIC-III dataset, we demonstrate the effectiveness of our framework in managing heterogeneous multimodal EHR data, reducing false positives and potentially improving the allocation of medical resources in the ICU.

While this paper focuses on binary classification tasks, many clinical applications require solutions for multiclass tasks (e.g., disease diagnosis) and continuous regression tasks (e.g., survival prediction). These are equally important and relevant for advancing clinical practice. In the future, we plan to expand our framework by incorporating additional data modalities, such as time series and medical images, to provide deeper clinical insights and enhance model performance. We also aim to extend the framework to handle multimodal EHR multiclass tasks, offering valuable predictive guidance for complex clinical scenarios. Additionally, we intend to investigate regression tasks, leveraging the recently introduced Epistemic Random Fuzzy Set (ERFS) theory [32, 33] and further building on developments in evidential regression [34].

ACKNOWLEDGMENTS

This research is supported by the National Research Foundation, Singapore under its AI Singapore Programme (AISG Award No: AISG-GC-2019-001-2B).

REFERENCES

1. Terwiesch C, KC D, Kahn JM. Working with capacity limitations: operations management in critical care. *Critical Care*. 2011;15:1-6.

2. Halpern NA, Pastores SM. Critical care medicine in the United States 2000–2005: an analysis of bed numbers, occupancy rates, payer mix, and costs. *Critical care medicine*. 2010;38(1):65-71.
3. Wang S, Jiang Y, Li Q, Zhang W. Timely ICU Outcome Prediction Utilizing Stochastic Signal Analysis and Machine Learning Techniques with Readily Available Vital Sign Data. *IEEE Journal of Biomedical and Health Informatics*. 2024.
4. Iwase S, Nakada Ta, Shimada T, Oami T, Shimazui T, Takahashi N, et al. Prediction algorithm for ICU mortality and length of stay using machine learning. *Scientific reports*. 2022;12(1):12912.
5. Ashrafi N, Liu Y, Xu X, Wang Y, Zhao Z, Pishgar M. Deep learning model utilization for mortality prediction in mechanically ventilated ICU patients. *Informatics in Medicine Unlocked*. 2024;49:101562.
6. Gao J, Lu Y, Ashrafi N, Domingo I, Alaei K, Pishgar M. Prediction of Sepsis Mortality in ICU patients using machine learning methods. *BMC Medical Informatics and Decision Making*. 2024;24(1):228.
7. Sheikhalishahi S, Miotto R, Dudley JT, Lavelli A, Rinaldi F, Osmani V, et al. Natural language processing of clinical notes on chronic diseases: systematic review. *JMIR medical informatics*. 2019;7(2):e12239.
8. Koleck TA, Tatonetti NP, Bakken S, Mitha S, Henderson MM, George M, et al. Identifying symptom information in clinical notes using natural language processing. *Nursing research*. 2021;70(3):173-83.
9. Oliwa T, Furner B, Schmitt J, Schneider J, Ridgway JP. Development of a predictive model for retention in HIV care using natural language processing of clinical notes. *Journal of the American Medical Informatics Association*. 2021;28(1):104-12.
10. Zhang D, Yin C, Zeng J, Yuan X, Zhang P. Combining structured and unstructured data for predictive models: a deep learning approach. *BMC medical informatics and decision making*. 2020;20:1-11.
11. Shin J, Li Y, Luo Y. Early prediction of mortality in critical care setting in sepsis patients using structured features and unstructured clinical notes. In: 2021 IEEE International Conference on Bioinformatics and Biomedicine (BIBM). IEEE; 2021. p. 2885-90.
12. Lin WC, Chen A, Song X, Weiskopf NG, Chiang MF, Hribar MR. Prediction of multiclass surgical outcomes in glaucoma using multimodal deep learning based on free-text operative notes and structured EHR data. *Journal of the American Medical Informatics Association*. 2024;31(2):456-64.
13. Johnson AE, Pollard TJ, Shen L, Lehman LwH, Feng M, Ghassemi M, et al. MIMIC-III, a freely accessible critical care database. *Scientific data*. 2016;3(1):1-9.
14. Liu V, Kipnis P, Gould MK, Escobar GJ. Length of stay predictions: improvements through the use of automated laboratory and comorbidity variables. *Medical care*. 2010;48(8):739-44.
15. Rajkomar A, Oren E, Chen K, Dai AM, Hajaj N, Hardt M, et al. Scalable and accurate deep learning with electronic health records. *NPJ digital medicine*. 2018;1(1):1-10.
16. Denoeux T. A neural network classifier based on Dempster-Shafer theory. *IEEE Transactions on Systems, Man, and Cybernetics-Part A: Systems and Humans*. 2000;30(2):131-50.
17. Shafer G. *A mathematical theory of evidence*. vol. 42. Princeton university press; 1976.

18. Dempster AP. Upper and lower probabilities induced by a multivalued mapping. In: *Classic works of the Dempster-Shafer theory of belief functions*. Springer; 2008. p. 57-72.
19. Lian C, Ruan S, Denœux T, Li H, Vera P. Joint tumor segmentation in PET-CT images using co-clustering and fusion based on belief functions. *IEEE Transactions on Image Processing*. 2018;28(2):755-66.
20. Huang L, Ruan S, Decazes P, Denœux T. Lymphoma segmentation from 3D PET-CT images using a deep evidential network. *International Journal of Approximate Reasoning*. 2022;149:39-60.
21. Huang L, Denœux T, Vera P, Ruan S. Evidence fusion with contextual discounting for multi-modality medical image segmentation. In: *International Conference on Medical Image Computing and Computer-Assisted Intervention*. Springer; 2022. p. 401-11.
22. Huang L, Ruan S, Decazes P, Denœux T. Deep evidential fusion with uncertainty quantification and reliability learning for multimodal medical image segmentation. *Information Fusion*. 2025;113:102648.
23. Gorishniy Y, Rubachev I, Khrulkov V, Babenko A. Revisiting deep learning models for tabular data. *Advances in Neural Information Processing Systems*. 2021;34:18932-43.
24. Devlin J. Bert: Pre-training of deep bidirectional transformers for language understanding. *arXiv preprint arXiv:181004805*. 2018.
25. Alsentzer E, Murphy JR, Boag W, Weng WH, Jin D, Naumann T, et al. Publicly available clinical BERT embeddings. *arXiv preprint arXiv:190403323*. 2019.
26. Breiman L. Random forests. *Machine learning*. 2001;45:5-32.
27. He K, Zhang X, Ren S, Sun J. Deep residual learning for image recognition. In: *Proceedings of the IEEE conference on computer vision and pattern recognition*; 2016. p. 770-8.
28. Wolf T. Huggingface's transformers: State-of-the-art natural language processing. *arXiv preprint arXiv:191003771*. 2019.
29. Lee J, Yoon W, Kim S, Kim D, Kim S, So CH, et al. BioBERT: a pre-trained biomedical language representation model for biomedical text mining. *Bioinformatics*. 2020;36(4):1234-40.
30. Pedregosa F, Varoquaux G, Gramfort A, Michel V, Thirion B, Grisel O, et al. Scikit-learn: Machine learning in Python. *the Journal of machine Learning research*. 2011;12:2825-30.
31. Paszke A, Gross S, Massa F, Lerer A, Bradbury J, Chanan G, et al. Pytorch: An imperative style, high-performance deep learning library. *Advances in neural information processing systems*. 2019;32.
32. Denœux T. Belief functions induced by random fuzzy sets: A general framework for representing uncertain and fuzzy evidence. *Fuzzy Sets and Systems*. 2021;424:63-91.
33. Denœux T. Reasoning with fuzzy and uncertain evidence using epistemic random fuzzy sets: General framework and practical models. *Fuzzy Sets and Systems*. 2023;453:1-36.
34. Huang L, Xing Y, Mishra S, Denœux T, Feng M. Evidential time-to-event prediction model with well-calibrated uncertainty estimation. *arXiv preprint arXiv:241107853*. 2024.
35. Smets P, Kennes R. The Transferable Belief Model. *Artificial Intelligence*. 1994;66:191-243.

APPENDIX

A Dempster-Shafer (DS) Theory

Let $\Omega = \{\omega_1, \omega_2, \dots, \omega_M\}$ be a finite set of hypotheses about some question, called the *frame of discernment*. Evidence about a variable taking values in Ω can be represented by a *mass function*: 2^Ω to $[0,1]$ such that $m(\emptyset) = 0$ and

$$\sum_{A \subseteq \Omega} m(A) = 1. \quad (1)$$

For any hypothesis $A \subseteq \Omega$, the quantity $m(A)$ is interpreted as a share of a unit mass of belief allocated to the hypothesis that the truth is in A , and which cannot be allocated to any strict subset of A based on the available evidence. Set A is called a *focal set* of m if $m(A) > 0$. A mass function is said to be Bayesian if its focal sets are singletons, and logical if it has only one focal set. Two mass functions m_1 and m_2 representing independent items of evidence can be combined conjunctively by *Dempster's combination rule* [17] \oplus as

$$(m_1 \oplus m_2)(A) = \frac{\sum_{B \cap C = A} m_1(B)m_2(C)}{1 - \sum_{B \cap C = \emptyset} m_1(B)m_2(C)}, \quad (2)$$

for all $A \neq \emptyset$, where $\sum_{B \cap C = \emptyset} m_1(B)m_2(C)$ is the degree of conflict among the two pieces of evidence, The nice information fusion attribute of DS theory points out the high potential of using DS theory for heterogenetic medical data analysis.

After aggregating all available evidence, we adopt the pignistic transformation, as proposed by Smets in the Transferable Belief Model [35], to make a final decision based on the combined mass function. This framework bases decisions on the pignistic probability distribution with the following expression:

$$p(\omega) = \sum_{A \subseteq \Omega: \omega \in A} \frac{m(A)}{|A|}, \forall \omega \in \Omega. \quad (3)$$

B Evidence mapping (EM)

As illustrated in Figure 6, the evidence mapping module consists of one input layer, one hidden layer, and one output layer. The input layer is composed of H units (H is the number of prototypes), whose weights vectors are prototypes $\pi_1, \pi_2, \dots, \pi_H$ in input space. The activation of unit h in the input layer is

$$s_h = \beta_h \exp(-\gamma_h d_h^2), \quad (4)$$

where $d_h = \|x - \pi_h\|$ denotes the Euclidean distance between input vector x and prototype π_h , $\gamma_h > 0$ is a scale parameter, and $\beta_h \in [0, 1]$ is an extra parameter. The hidden layer computes mass functions m_h (evidence) of each

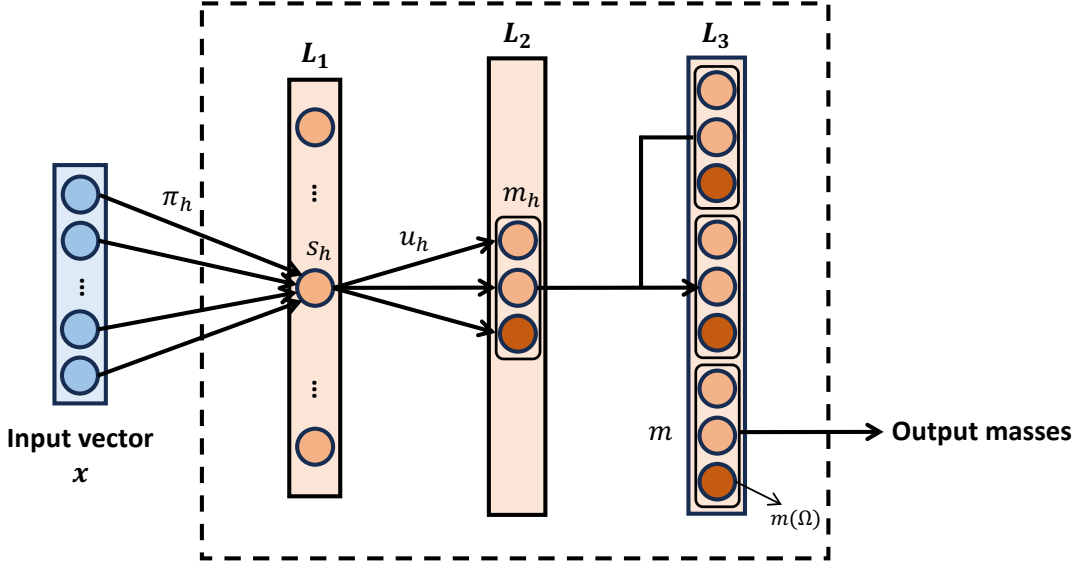


Figure 6: The illustration of evidence mapping

prototype π_h is defined as:

$$m_h(\{\omega_c\}) = u_h^{(c)} s_h, \quad c = 1, 2, \dots, M, \quad (5a)$$

$$m_h(\Omega) = 1 - s_h, \quad (5b)$$

where $u_h^{(c)}$ is the membership degree of prototype h to class ω_c , $\sum_{c=1}^M u_h^{(c)} = 1$, and M is the number of classes. Therefore, the vector of mass functions induced by prototypes is denoted as:

$$m_h = (m_h(\{\omega_1\}), m_h(\{\omega_2\}), \dots, m_h(\{\omega_M\}), m_h(\Omega)) \in \mathbb{R}^{M+1}. \quad (6)$$

Finally, the mass functions are then aggregated by Dempster's combination rule using Eq. 2 in the output layer. A combined mass function m is computed as the orthogonal sum of the H mass functions:

$$m = m_1 \oplus m_2 \oplus \dots \oplus m_H \in \mathbb{R}^{M+1}. \quad (7)$$

The combined mass functions (the outputs of the EM module) represent the degrees of belief about the given class with $m(\{\omega_c\})$, as well as its prediction uncertainty with $m(\Omega)$. In our binary classification case, the dimension of EM module outputs would be three.

C Evidence fusion

To combine multiple mass functions m_1, m_2, \dots, m_K from different modalities/data types/data sources, Dempster's combination rule is applied again Eq. 2 to aggregate evidence for multiple sources for final evidence generation.

$$m = m_1 \oplus m_2 \oplus \dots \oplus m_K \in \mathbb{R}^{M+1}, \quad (8)$$

where K is the number of mass functions to combine. For example, $K=2$ for the fusion of evidence from structured EHRs and free-text notes.

D The details of augmented learning algorithm

Let $p_i = (p_i(\omega_1), \dots, p_i(\omega_c), \dots, p_i(\omega_M))$ be the final probability after the pignistic transformation (3) for training sample i , and $y_i = (y_{i,1}, y_{i,2}, \dots, y_{i,M})$ denotes the one-hot encoding for corresponding ground-truth labels. The main loss function \mathcal{L}_{main} is computed as:

$$\mathcal{L}_p = -\frac{1}{N} \sum_{i=1}^N \sum_{c=1}^M w_c y_{i,c} \log(p_i(\omega_c)), \quad (9)$$

where N is the number of training samples, M denotes the number of classes, and w_c is the weight assigned to each class to address the class imbalance issue.

Moreover, two auxiliary cross-entropy losses are introduced to optimize the feature representation performance of the encoders, as the evidence mapping module performs more effectively with high-quality representations. Firstly, to regulate the representation generated by encoders, we added an additional fully connected network (FCN) to generate logits o_i for each modality. Let $o_i^s = (o_{i,1}^s, o_{i,2}^s, \dots, o_{i,M}^s)$ and $o_i^n = (o_{i,1}^n, o_{i,2}^n, \dots, o_{i,M}^n)$ be the logits from the encoders for structured data and free-text notes, respectively, the cross-entropy losses \mathcal{L}_{aux}^s and \mathcal{L}_{aux}^n are then calculated with y_i for structured data and notes, respectively:

$$\mathcal{L}_{aux}^s = -\frac{1}{N} \sum_{i=1}^N \sum_{c=1}^M w_c y_{i,c} \log \frac{\exp(o_{i,c}^s)}{\sum_{b=1}^M \exp(o_{i,b}^s)}, \quad (10)$$

$$\mathcal{L}_{aux}^n = -\frac{1}{N} \sum_{i=1}^N \sum_{c=1}^M w_c y_{i,c} \log \frac{\exp(o_{i,c}^n)}{\sum_{b=1}^M \exp(o_{i,b}^n)}, \quad (11)$$

Ultimately, the overall loss function $\mathcal{L}_{overall}$ is defined as follows:

$$\mathcal{L}_{overall} = \mathcal{L}_{main} + \alpha \mathcal{L}_{aux}^s + \beta \mathcal{L}_{aux}^n, \quad (12)$$

where α, β are the hyperparameters that control the balance between the main loss and the auxiliary cross-entropy losses.

E The model comparison results in metrics (specificity, recall, sensitivity, and NPV)

Model	Structured	Notes	Precision \uparrow	Recall \uparrow	Specificity \uparrow	NPV \uparrow
Random Forest	x		0.2634 \pm 0.0014	0.6946 \pm 0.0037	0.7398 \pm 0.0015	0.9476 \pm 0.0006
MLP	x		0.2741 \pm 0.0023	0.7707 \pm 0.0045	0.7264 \pm 0.0047	0.9594 \pm 0.0005
ResNet	x		0.2809 \pm 0.0007	0.7676 \pm 0.0036	0.7367 \pm 0.0017	0.9594 \pm 0.0005
FT-Transformer	x		0.2838 \pm 0.0015	0.7832 \pm 0.0054	0.7352 \pm 0.0019	0.9620 \pm 0.0009
BERT		x	0.1767 \pm 0.0030	0.6966 \pm 0.0225	0.5634 \pm 0.0217	0.9330 \pm 0.0021
BioBERT		x	0.1793 \pm 0.0011	0.6029 \pm 0.0278	0.6299 \pm 0.0194	0.9225 \pm 0.0028
Clinical Bert		x	0.1962 \pm 0.0012	0.7158 \pm 0.0080	0.6071 \pm 0.0073	0.9410 \pm 0.0009
Multimodal (BERT)	x	x	0.2761 \pm 0.0034	0.7807 \pm 0.0063	0.7255 \pm 0.0064	0.9611 \pm 0.0008
Multimodal (BioBERT)	x	x	0.2741 \pm 0.0031	0.7934\pm0.0065	0.7182 \pm 0.0067	0.9629\pm0.0008
Multimodal (Clinical Bert)	x	x	0.2908 \pm 0.0027	0.7678 \pm 0.0063	0.7489 \pm 0.0054	0.9601 \pm 0.0008
Ours (MLP-BERT)	x	x	0.3297 \pm 0.0076	0.6957 \pm 0.0168	0.8094 \pm 0.0114	0.9522 \pm 0.0020
Ours (MLP-BioBERT)	x	x	<u>0.3377\pm0.0115</u>	0.6792 \pm 0.0218	<u>0.8191\pm0.0148</u>	0.9503 \pm 0.0023
Ours (MLP-Clinical Bert)	x	x	0.3609\pm0.0075	0.6478 \pm 0.0123	0.8454\pm0.0079	0.9472 \pm 0.0013
Ours (ResNet-BERT)	x	x	0.3179 \pm 0.0073	0.7206 \pm 0.0168	0.7916 \pm 0.0118	0.9550 \pm 0.0020
Ours (ResNet-BioBERT)	x	x	0.3244 \pm 0.0100	0.7092 \pm 0.0219	0.8000 \pm 0.0150	0.9538 \pm 0.0025
Ours (ResNet-Clinical Bert)	x	x	0.326 \pm 0.0067	0.7151 \pm 0.0131	0.8010 \pm 0.0097	0.9546 \pm 0.0015
Ours (FT-Trans-BERT)	x	x	0.3163 \pm 0.0080	0.7433 \pm 0.0109	0.7836 \pm 0.0110	0.9580 \pm 0.0012
Ours (FT-Trans-BioBERT)	x	x	0.3282 \pm 0.0015	0.7193 \pm 0.0055	0.8027 \pm 0.0027	0.9553 \pm 0.0007
Ours (FT-Trans-Clinical Bert)	x	x	0.3289 \pm 0.0070	0.7371 \pm 0.0171	0.7974 \pm 0.0108	0.9578 \pm 0.0021

(a) Mortality prediction

Model	Structured	Notes	Precision \uparrow	Recall \uparrow	Specificity \uparrow	NPV \uparrow
Random Forest	x		0.2360 \pm 0.0045	0.6744 \pm 0.0131	0.6616 \pm 0.0150	0.9295 \pm 0.0014
MLP	x		0.2615 \pm 0.0013	0.6542 \pm 0.0034	0.7147 \pm 0.0030	0.9305 \pm 0.0004
ResNet	x		0.2673 \pm 0.0016	0.6420 \pm 0.0039	0.7282 \pm 0.0025	0.9295 \pm 0.0006
FT-Transformer	x		0.2603 \pm 0.0026	0.6974 \pm 0.0061	0.6938 \pm 0.0067	0.9369 \pm 0.0007
BERT		x	0.2004 \pm 0.0031	0.5685 \pm 0.0147	0.6488 \pm 0.0160	0.9070 \pm 0.0009
BioBERT		x	0.2006 \pm 0.0022	0.5504 \pm 0.0160	0.6610 \pm 0.0141	0.9051 \pm 0.0013
Clinical Bert		x	0.2208 \pm 0.0024	0.6251 \pm 0.0133	0.6587 \pm 0.0116	0.9193 \pm 0.0014
Multimodal (BERT)	x	x	0.2568 \pm 0.0029	0.6892 \pm 0.0141	0.6915 \pm 0.0108	0.9347 \pm 0.0022
Multimodal (BioBERT)	x	x	0.2554 \pm 0.0034	0.6943 \pm 0.0136	0.6868 \pm 0.0114	0.9358 \pm 0.0018
Multimodal (Clinical Bert)	x	x	0.2507 \pm 0.0045	0.7201\pm0.0188	0.6664 \pm 0.0163	0.9394 \pm 0.0024
Ours (MLP-BERT)	x	x	0.2809 \pm 0.0038	0.6218 \pm 0.0050	0.7538 \pm 0.0064	0.9281 \pm 0.0005
Ours (MLP-BioBERT)	x	x	0.2892 \pm 0.0048	0.6022 \pm 0.0061	0.7710 \pm 0.0071	0.9262 \pm 0.0007
Ours (MLP-Clinical Bert)	x	x	0.2980\pm0.0075	0.5899 \pm 0.0134	0.7841\pm0.0117	0.9254 \pm 0.0012
Ours (ResNet-BERT)	x	x	0.2787 \pm 0.0071	0.6460 \pm 0.0158	0.7402 \pm 0.0148	0.9314 \pm 0.0016
Ours (ResNet-BioBERT)	x	x	0.2848 \pm 0.0059	0.6212 \pm 0.0126	0.7580 \pm 0.0119	0.9285 \pm 0.0012
Ours (ResNet-Clinical Bert)	x	x	<u>0.2968\pm0.0029</u>	0.6227 \pm 0.0073	<u>0.7720\pm0.0058</u>	0.9299 \pm 0.0008
Ours (FT-Trans-BERT)	x	x	0.2595 \pm 0.0036	<u>0.7180\pm0.0116</u>	0.6830 \pm 0.0110	0.9402\pm0.0014
Ours (FT-Trans-BioBERT)	x	x	0.2668 \pm 0.0042	0.6914 \pm 0.0106	0.7059 \pm 0.0109	0.9368 \pm 0.0012
Ours (FT-Trans-Clinical Bert)	x	x	0.2782 \pm 0.0026	0.6766 \pm 0.0046	0.7288 \pm 0.0050	0.9359 \pm 0.0005

(b) PLOS prediction

Table 3: The model comparison for mortality (a) and PLOS prediction (b) tasks in metrics (precision, recall, specificity, and NPV).

F The evaluation on different fusion settings for PLOS prediction

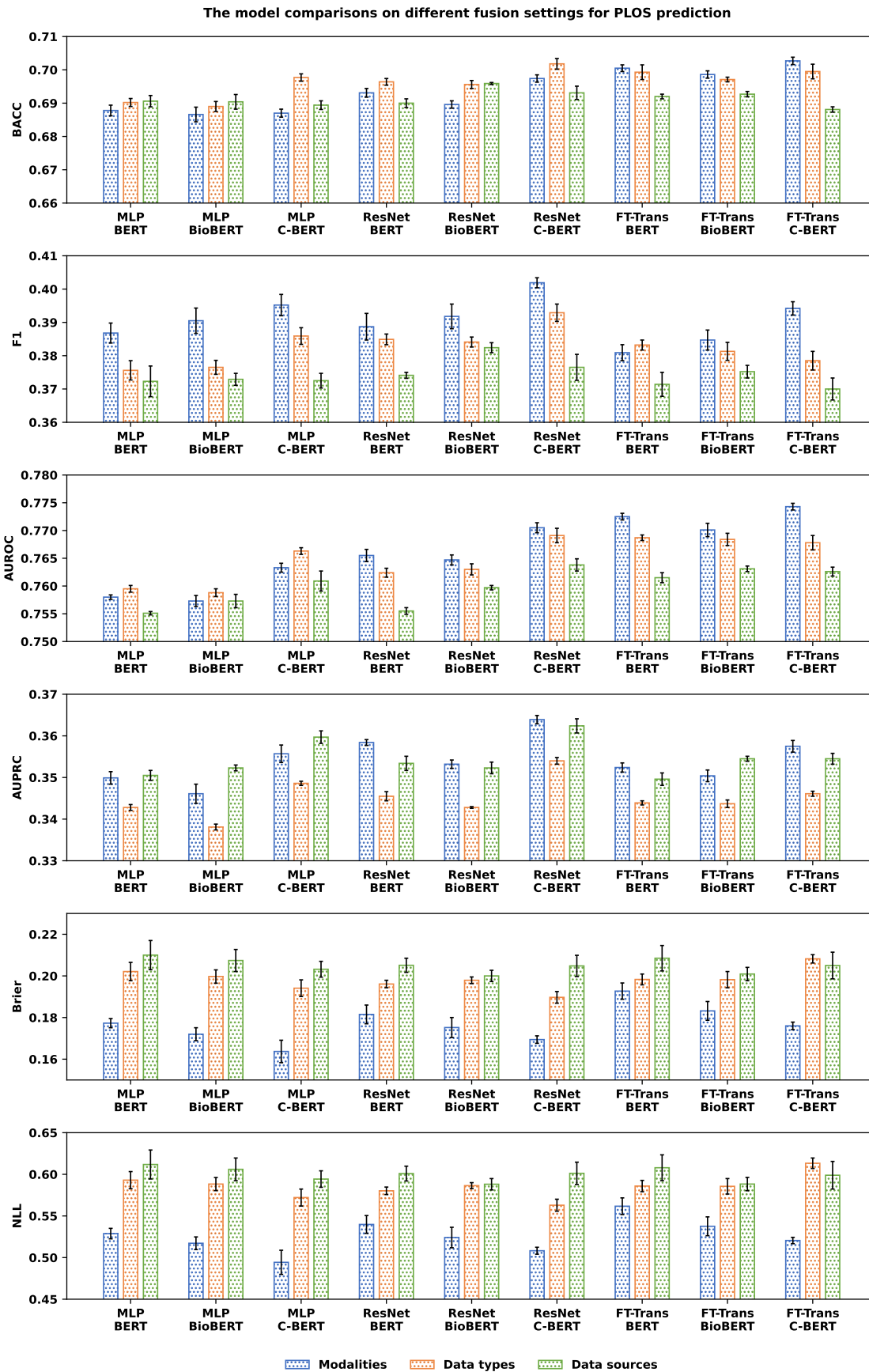


Figure 7: The evaluation of our framework on different fusion settings for PLOS prediction: (1) modalities, (2) data types, (3) data sources.